Mechanical-chemical coupling in Temporomandibular Joint disc

Rodney Marcelo Do Nascimento, Adrien Baldit, Ninel Kokanyan, Lara Kristin Tappert, Paul Lipinski, Antonio Carlos Hernandes, Rachid Rahouadj

Mechanical-Chemical Coupling in Temporomandibular Joint Disc

Rodney Marcelo do Nascimento[1,2,5], Adrien Baldit[2], Ninel Kokanyan[3,4], Lara Kristin Tappert[2], Paul Lipinski[2], Antônio Carlos Hernandes[1], Rachid Rahouadj[2]

(1) São Carlos Institute of Physics, University of São Paulo, USP, Brazil

(2) Mécanique des Matériaux, des Structures et du Vivant, LEM3, CNRS, Université of Lorraine, France

(3) Laboratoire Matériaux Optiques, Photonique et Systèmes (LMOPS), Centrale Supélec, Université Paris-Saclay, 2 rue E. Belin, 57070 Metz, France

(4) Université de Lorraine, Laboratoire Matériaux Optiques, Photonique et Systèmes (LMOPS), EA-4423, 2 rue E. Belin, 57070, Metz, France

(5) Universidade Federal de Santa Catarina, UFSC, Brazil

ABSTRACT

This paper reports an experimental investigation based on vibrational spectroscopy of biological materials by a new custom-made device allowing simultaneously applying tensile load with changes within a controlled chemical environment. The response of the molecular structures of Temporomandibular Joint (TMJ) discs under simulated daily mechanical stimulations was characterized by stress-strain analysis and Raman spectra. The results show that changes in the biochemical environment around tissue (associated to common disorders) led to significant modifications to its mechanical properties. The molecular response to stress was then fully characterized by a combination of molecular mapping followed by statistical analysis via Principal Component Analysis resulting in the identification of the phenylalanine-aromatic amino acids as a significant mechanical-chemical effector of TMJ discs. The coupled tensile machine and vibrational spectroscopy approach enabling *in-situ* molecular studies proves to be a powerful technique for biological material characterization and tissue engineering.

Keywords: biological material, mechanical stress, chemical environment, molecular mapping, temporomandibular disc, tissue engineering.

1. INTRODUCTION

Temporomandibular joint (TMJ) disc, located between the temporal bone and the mandibular condyle, is a biological material categorized as a fibrocartilage tissue, composed mainly of collagen

fibers (especially Collagen type I), which play an important role in TMJ disc's tensile properties [1, 2]. The TMJ discs are responsible for the basic human activities, such as mastication and phonation, and is, however, one of the most difficult cartilages to replace. Besides, it exhibits a limited ability to heal. Both biomechanical and biochemical environment of the material are responsible for renewing, degradability and regeneration of the tissue [1]. Despite advances in the material science of TMJ discs, the response of each biomolecular group to the daily mechanical stresses taking into account the effects of the chemical environment on its viscoelastic properties has not yet been established.

The strain field of the TMJ disc is a result of stress from different origins, e.g., tensile [3, 4], compression [5, 6] and friction [7, 8] due to daily mechanical loads. The mechanical stresses in daily motions involve extrinsic parameters, such as their amplitude and frequency, and intrinsic parameters, such as molecular structure and biological environment. A modification of those parameters, voluntary or not, generates a global modification at the macroscopic scale of the biological material [9-11]. Large damage of the TMJ disc does not heal over time because the cartilage cannot recover due to its non-vascularizing characteristic [12]. The irrigation of tissue, the biochemical interactions and ionic diffusion are triggered by osmosis through the extracellular fluid. For this reason, the chemical environment concerning the body fluid has an important role in tissue degradability and regeneration. For instance, studies have shown the effects of mineralization processes on the biomechanical properties of articular cartilages [13, 14]. In particular, calcium phosphates aggregated on tissue appears to reduce the ability of the cartilage to support mechanical loads and may contribute to the development of degenerative changes of the articular cartilage [15]. An additional and recurring concern is related to the metabolically driven processes in cartilage degeneration. Conditions of prolonged oxidative stress, which occur during chronic inflammation, can induce biochemical changes in cartilage structural resulting in degradation and impairing the ability of the biomaterial to withstand mechanical stresses [16,17]. Few attempts have been made to create an inflammation simulating the pathological chemical environment of the diseased joint in order to study the molecular and mechanical changes associated with such an environment.

The need to establish an effective methodology capable to assess the molecular structure, mechanical

properties and effects of biochemical environment on the TMJ disc simultaneously is evident. A key approach to tackle this problem is the combination of stress-strain analysis and vibrational spectroscopy [18,19]. In particular, the use of Raman spectroscopy for *in situ* investigations on real soft tissue has demonstrated to be a powerful tool for an accurate molecular description [20]. Raman spectroscopy has real advantages for biomedical applications, as it is non-destructive, non-invasive, fast and provides information at the molecular and structural level. Moreover, as water produces low Raman scattering intensity, so it doesn't interfere with the Raman response of the sample under study. Raman spectroscopy, specially coupled with chemometrics, has various applications in biomedical field such as cancer diagnosis [21,22] and skin diseases [23]. Herein, we have designed an experimental bench using a micro tensile machine coupled to a confocal Raman microscope to investigate TMJ disc samples extracted from domestic pigs. Pigs are the most suitable animal model to compare with humans because human and porcine TMJ discs exhibit similar anatomy, size of articular structures and shape [24-26]. The biological medium regarding composition, pH and temperature was reproduced in the device around the disc and the results show the sensitivity of the tissue to the changes in the biochemical environment. Posteriorly, the molecular responses under daily mechanical stresses was fully characterized and statistical analysis followed in order to obtain the major contributors to the biomechanics of the TMJ disc. The chemo-mechanical coupling effect of TMJ discs assessed by this new approach is discussed in relation to successful (or unsuccessful) tissue response.

2. MATERIALS AND METHODS

2.1 Samples

Herein, both TMJ discs were harvested from the cadaver of a domestic pig race hybrid large white – (Landrace Pietran) obtained from a local slaughterhouse. The central part of the disc one was separated from the tissue bonder using a surgical knife. The region of interest is highlighted on the specimen quadrant presented in Figure 1.a. The specimens were separated into three parts (1, 2 and 3 regions of the disc) and excised in an anatomical cut in order to preserve the orientation of tissue fibers. The first part of the disc one was submitted to preliminary mechanical characterization, i.e., a fresh sample

(labelled TMJ#1), while the remaining parts of the disc were stored in a 0.15 mol.L^{-1} NaCl solution in a freezer until the subsequent tests. The second disc was stored in the same solution in a freezer until the Raman-mapping. The second part of the disc one (labelled TMJ#2) was characterized and then incubated in a simulated body fluid (SBF). This sample was immersed in wells containing 5 ml of SBF, kept at 37.5°C for 15 days. The biological fluid was renewed every 3 days. After the time interval, the sample was collected, gently cleaned in ultrapure water and investigated by Raman spectroscopy and stress-strain analysis in a renewed body fluid. In order to investigate the effects of changes in the biological environment on the TMJ disc, the third part of the disc one (labeled TMJ#3) was exposed to an oxidative chemical environment for different periods, i.e., 1 min, 10 h and 2 days and were also characterized by Raman spectroscopy and stress-strain analysis. A part of disc two (labeled TMJ#4) was exclusively used for Raman Mapping experiments and Multivariational analysis. For each experiment, the samples were fixed to the device grips in the micro tensile machine with constant hydration. The average dimensions of the samples, characterized by length *l*, width *w* and thickness *t*, were measured through a digital calliper. The obtained values in sample location are gathered in table 1.

Table 1 – Average dimensions of the TMJ disc samples

Sample	**Sample Location**	***l* (mm)**	***w* (mm)**	***t* (mm)**
TMJ#1	**1**	**10**	**4**	**1.5**
TMJ#2	**2**	**9**	**4**	**2**
TMJ#3	**3**	**7.5**	**4.1**	**2.3**
TMJ#4	**1**	**9**	**4**	**2**

2.2 Experimental bench

The experimental stress-strain analysis of the TMJ disc was done by a new homemade hydro-chemo-mechanical device illustrated in Figure 1.b. The device was coupled with a Raman spectroscope allowing simultaneous molecular characterization as function of the chemical environment. An example of screen output of the program used for the monitoring of force, temperature, pH and O_2 over time inside the hydro-chemo-mechanical device is provided in the supporting information. The individual

parts of this approach are detailed as follows:

- Device for tensile test: The experiment consisted of performing uniaxial tensile tests in the range of 0.25-30 N of applied forces. Measuring the displacement and tensile force as function of the time, the mechanical response was obtained in terms of stress relaxation and elastic modulus. The system remained closed during all experiments in order to avoid external perturbation. The interior of the bath is made of stainless steel with a micro device that allows the alteration of components of different types of metals, e.g., titanium, iron or copper. The bath is also equipped with a set of sensors, including force, O_2 and pH sensors. The latter two allow the modification and monitoring of the chemical environment changing the fluid circulation. To characterize the mechanical behaviour of the TMJ disc tissue, an elastic modulus, $E = \Delta\sigma / \Delta\varepsilon$, was evaluated by linear regression at the final of loading stress (σ) - strain (ε) curve. After finishing the mechanical load, the sample was submitted to its initial condition (without stress) and a second experiment was performed after 30 minutes of tissue relaxation/equilibration to reproduce the stress-strain curve.

- Chemical Environment: Simulated body fluid (SBF) medium was obtained by the dissolution of chemical reagents in 1 L of ultrapure distilled water. The reagents were dissolved one by one using magnetic stirring in the following order: sodium chloride (NaCl), sodium hydrogen carbonate ($NaHCO_3$), potassium chloride (KCl), di-potassium hydrogen phosphate trihydrate ($K_2HPO_4.3H_2O$), magnesium chloride hexahydrate ($MgCl_2.6H_2O$), calcium chloride ($CaCl_2$), sodium sulfate (Na_2SO_4) and Tris-hydroxymethyl aminomethane ($(HOCH_2)3CNH_2$). The temperature and pH were adjusted to 36.5 ± 0.5 and 7.45 ± 0.02, respectively. This procedure was established to obtain the same chemical composition as blood's plasmas [27]. The SBF medium was sterilized under UV light for 15 min before insertion in the bioreactor. Further, we have simulated oxidative stress to be closer to chronic inflammatory and degenerative conditions of cartilage tissues by biochemical environment change. For the system control, a pair of sensors inside the bioreactor and close to the samples measured the concentration of O_2 and the pH evolution over time (Figure 1.b).

-Vibrational Spectroscopy: the high spatial resolution and non-destructive specificity of the Raman

spectroscopy were used to capture the tissue composition at molecular scales. The studies were carried out at the Laboratoire des Matériaux Optiques, Photonique et Systèmes (LMOPS), Centrale Supélec/Université de Lorraine. Confocal spectroscopy and spectral mapping were employed to probe the phase of the tissues through XYZ profiles of the vibrational bands. The spectra and the Raman spectral mapping were obtained by using a LabRAM HR Evolution (*Horiba*) microscope confocal Raman spectrometer equipped with a linear stage, piezo-driven, 50x objective lens (*Olympus*). The excitation line of 785 nm wavelengths and the backscattered configuration were used. The chemical morphologies and structure of the TMJ samples were investigated by Raman mappings from XY profiles carried out in a region of 2 x 2 μm^2 and 5 x 5 μm^2. The integration time for each point was 1.5 s and mapping was carried out at room temperature. A hydro-chemo-mechanical device coupled to the confocal Raman microscope was designed seeking *in situ* molecular analysis under tensile load. The lens of the microscope was positioned perpendicular to the tensile direction to observe both transverse planes. Figure 1.c shows an image of the device coupled to a confocal Raman microscope.

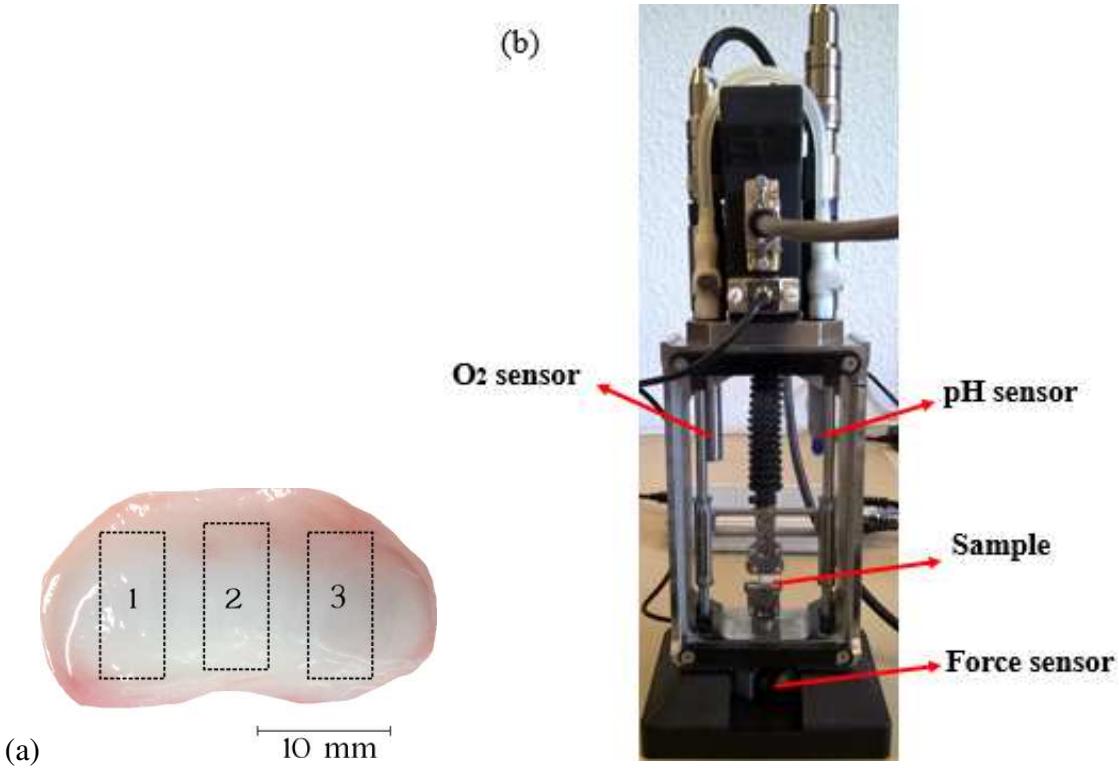

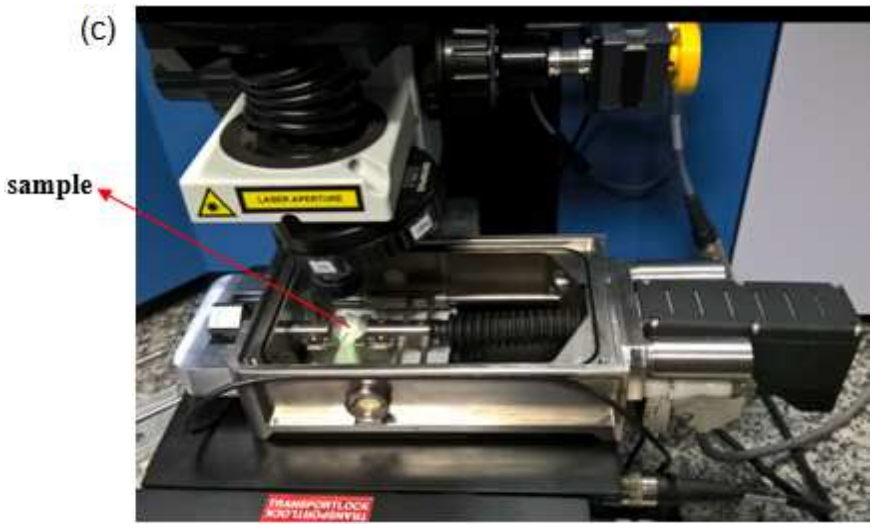

Figure 1- TMJ disc sample extracted from pig cadaver (the region of interest is highlighted) (a); photography of the hydro-chemo-mechanical device in a vertical set (b), and the photograph of the device coupled to a confocal Raman microscope (c).

2.3 Simulation of the daily mechanical load with the micro tensile test machine

Our mechanical simulation using the TMJ disc as a model system was based on the anatomy of a cadaver obtained from real kinematics [28] as illustrated in the sequential image of Figure 2.a with its respective displacement vector (red lines) reproduced in Figure 2.b. The vectors represent the displacement of the centre of the bony part of the top (1) relative to the bony part of the underside (2). The representation of the displacement field (red lines) is based on one cycle of the daily mechanical load with the hypothesis that all cycles exhibit the same displacement, as we have stated 10% of displacement for our experiments. In fact, the kinematics of the TMJ disc includes rotation and translation, rotation relative to the transcranial axis and translation relative to the skull base. Three types of loading occur during daily mechanical load: compression, tension and shear, which may be static for instance during clenching or dynamic while chewing. In our approach, we deal with only tensile properties of the TMJ disc during loading. Furthermore, to adapt the kinematic of the daily mechanical stress, the samples were preconditioned for 5 loading-unloading cycles in the tensile machine followed by the stress relaxation phase during which the measurements were performed. Figure 2.c shows the loading sequence applied to TMJ disc sample by the micro tensile machine. The tensile tests were applied to the antero-posterior direction at the intermediate zone of the samples. The tensile loadings

were carried out at a rate of 0.01 mm/s (representing a time cycle as we have stated for our experiment), to reach an engineering strain of 10% elongation of the original length *l* in order to remain in a physiological loading condition and a low viscous effect. At least five measurements were performed on each sample. The Raman spectroscopy was performed on samples before and after mechanical stresses, considering the last loading after stress relaxation.

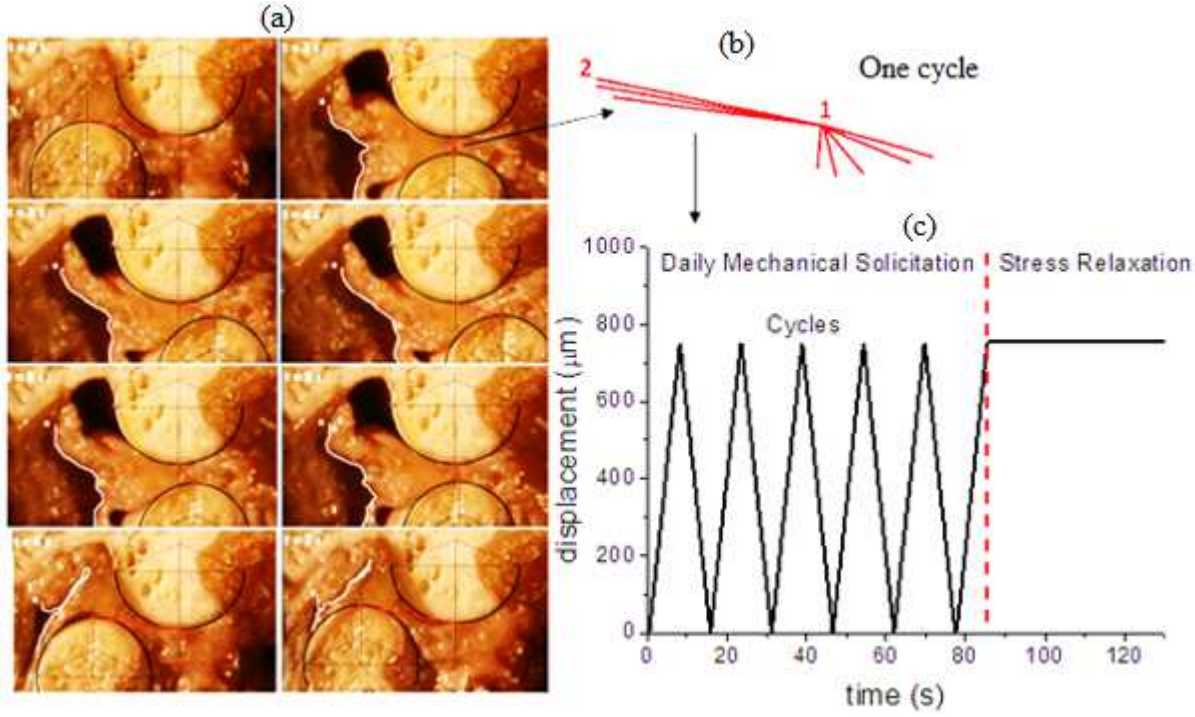

Figure 2- Sequential images of the kinematic of a TMJ (a) from a cadaver adapted from ref. [28] with the representation of the displacement during a cycle (b) and the reproduction of the cyclic movements followed by a constant position during stress relaxation (c).

2.4 Raman mapping and statistical analysis

The Raman spectra were treated through the subtraction of the baseline and Lorentzian deconvolution of the peaks. For Raman-mapping, we applied Principal Component Analysis (PCA) in order to obtain significant and statistical variations of the complex dataset of multiple dimensions by assessing the molecular structures and their spatial distribution at the micron level. From Raman spectra, we extracted a set of spectrum in 3x5 µm to create a molecular map by converting XY data into matrix analysis. In order to resolve the spectral components that are present in different proportions in the TMJ tissue, the

dimensionalities were reduced by an alternative set of coordinates in a general format [29-32], at hand given by:

$$X = TP^T + E$$

where the matrix X is decomposed by PCA into two smaller matrices, T and P, named scores and loadings, respectively. E is the residuals of X. Our principal component is, therefore, the linear combination of the original variables, which transform the large number of Raman shifts related to different molecular structure of the tissue into a smaller number of uncorrelated variables according to the necessary numerical condition:

$$\sum_{i=1}^{I} t_{ia}\ t_{ib} = 0\,;\ \sum_{i=1}^{I} p_{ia}\ p_{ib} = 0$$

where t_a and, t_b are the a^{th} and b^{th} columns of T matrix, respectively while p_a and p_b are the a^{th} and b^{th} rows of P matrix, respectively. The order of the principal components (PCs) denoted their importance to the dataset of the spectra. For instance, PC1 described the highest amount of variation, PC2 the second highest, and so on, which provided insight into the percentage of variance in the molecular complexity of the TMJ tissue. All PC-loadings were plotted as a function of the Raman shifts.

3. RESULTS

3.1 Mechanical and molecular characterization of the TMJ disc

Figure 3.a shows the force and displacement as a function of the time obtained for five cycles at a 0.1 mm/s displacement rate and Figure 3.b shows the stress-strain curves for TMJ samples obtained from the antero-posterior direction. The mechanical behaviour of the tissue is characterized by successive linear and non-linear regimes. A similar behaviour was observed in other TMJ samples at 20% and 30% strain. In addition, a stress-strain stabilization between the first and the fifth cycles is observed, which can be attributed to sample conditioning upon daily mechanical load. From the results for each cycle, we obtained an elastic modulus E equal to 4.0 ± 0.5 MPa for a fresh sample TMJ#1. For comparisons, Young's modulus close to 8 MPa in samples stored in a freezer was obtained by our group

using a disc from the same animal [33], and at the same strain rate.

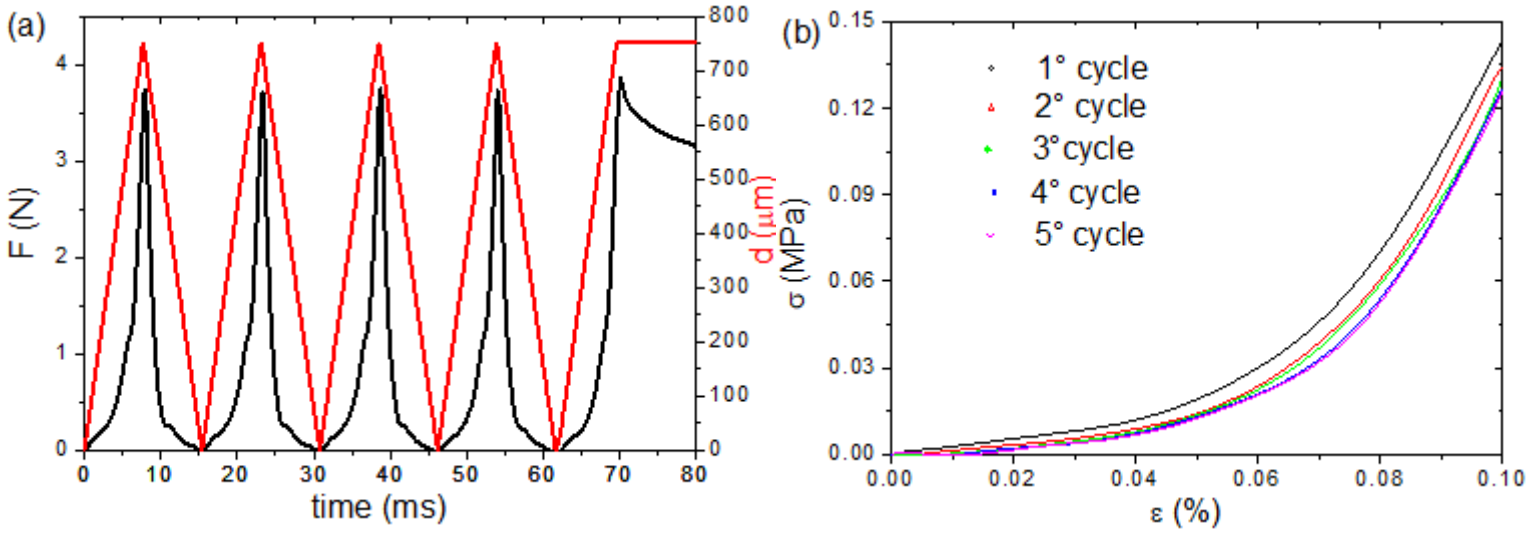

Figure 3- Mechanical characterization of TMJ#1 sample: typical result of force and displacement as function of time (a) and stress-strain (b) of a fresh TMJ sample measured during five cycles.

Figure 4.a displays the Raman spectra acquired from TMJ#1 by using λ = 785 nm excitation, at room temperature. The Lorentzian decomposition suggests at least 21 different chemical groups that characterize the complexity of the molecular structure of the TMJ tissue. The main peaks investigated in this study are identified in the figure inset. The description of the positions and assignments of bands of macromolecules observed in Raman spectra of the TMJ sample based on literature reports are provided in supplementary table 1. The Raman spectra exhibited the characteristic peaks of macromolecular structure, along with peaks related to the existence of collagens, the main component of the TMJ disc extracellular matrix [1]. For instance, the band in the 1620-1700 cm^{-1} spectral range is assigned to C=O stretching rocking, a characteristic of the amide I-phase, one of the secondary molecular structures observed in 80% of proteins. This spectral region also exhibits C=C stretching, characteristic vibration of hydrocarbons. The bands in the 1410-1480 cm^{-1} region are assigned to C-H deformation from organic content. Bands related to proteoglycan structures were identified for 1370-1380 cm^{-1} range while bands observed in the 995-1005 cm^{-1} region are attributed to the breathing mode of the phenylalanine-aromatic amino acids. Figure 4.b shows the Raman spectra of TMJ samples before and after mechanical solicitation. In some spectra, there is a slight shift towards higher frequencies after

mechanical loading. This was noticed, in particular, in regions with low wavenumber. The Raman signal is sensitive to local strain, such as C-C stretch in the 930-950 cm^{-1} range. From the results, strain appears to induce shifts in vibrational frequencies. However, the complexity of the local stress/strain molecular distribution of TMJ tissue observed in, at least 21 chemical groups, is not evident, therefore necessitating appropriate statistical analysis based on Raman-mapping, as will be reported later.

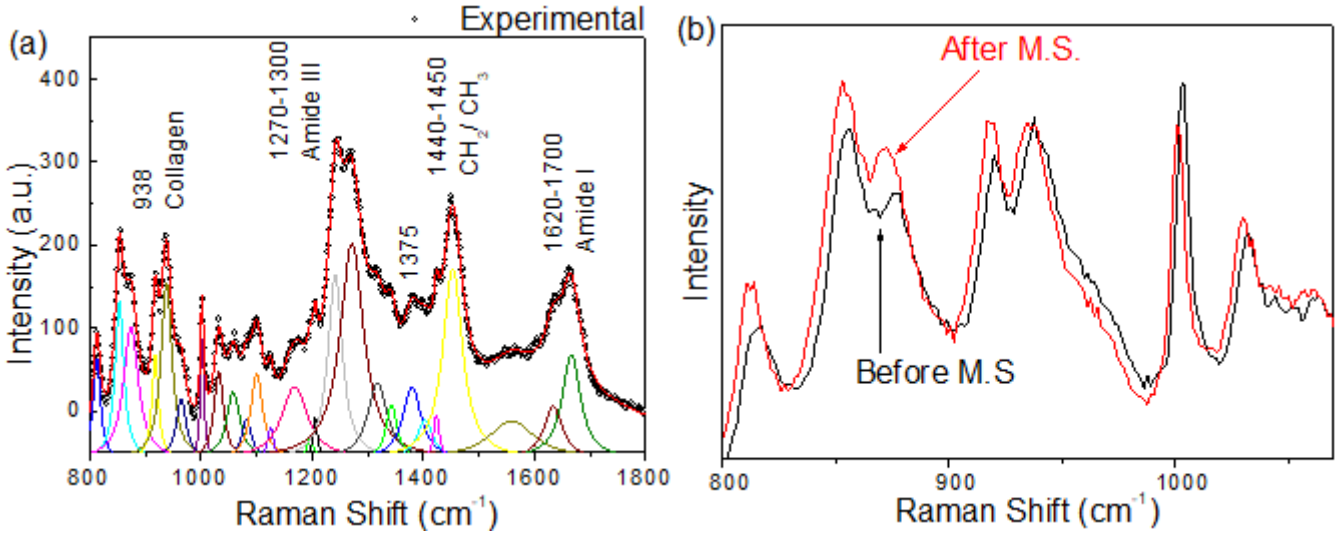

Figure 4- Line shape analyses of the Raman spectra and main molecular assignment (after baseline correction) (a); Low region Raman shift before and after mechanical stressing (M.S). (b).

3.2 Effects of the SBF saturation on mechanical properties and Raman spectra

Figure 5.a shows the stress versus strain for TMJ#2 obtained from the fifth cycle of daily mechanical loading after 15 days of the incubation process in comparison with a control sample, i.e., before incubation in SBF. The stress versus strain for TMJ#2 increased significantly at a strain of 10% with elastic modulus changing from ≈ 8 to ≈ 27 MPa. The evolution of the stress as function of normalized time is represented in Figure 5.b, for each tested sample. The time to steady-state after the relaxation process is similar in each case, as shown in the figure inset Figure 5.b, thus suggesting the material preserves its "molecular memory" for stress relaxation possibly attributed to specific chemical groups related to elastic protein material, such as amides. Figure 5.c displays the Raman spectra of the TMJ#2 before and after the incubation process in simulated body fluid acquired by using λ = 782 nm excitation, at room temperature. A significant spectral region modification is observed in the 950-980 cm^{-1} range.

The presence of the saturated colloidal solution (SBF environment) seems to affect molecular groups of the tissue matrix. This assignment is characteristic of structures related to calcium phosphate vibrational modes, $\nu_1PO_4^{3-}$ present in the bone mineral structures containing extensive HPO_4^{2-}, usually immature [34]. In particular, such region is associated with internal vibrations of the PO_4 unit. Fig. 5.d shows the line shape analyses of the Raman spectra before and after the incubation process. For the first condition, spectral fit converges to 4 shift peaks before the incubation process while spectral fit converge to 8 shift peaks after the incubation process. The revelation of additional peaks at those regions indicates the formation of a phosphate band ($\nu_1PO_4^{3-}$), which is characteristic of carbonated apatites. Taken together, the results from Figures 5.a-d identify these key mediators related to calcium absorption in affecting the mechanical properties of the TMJ disc.

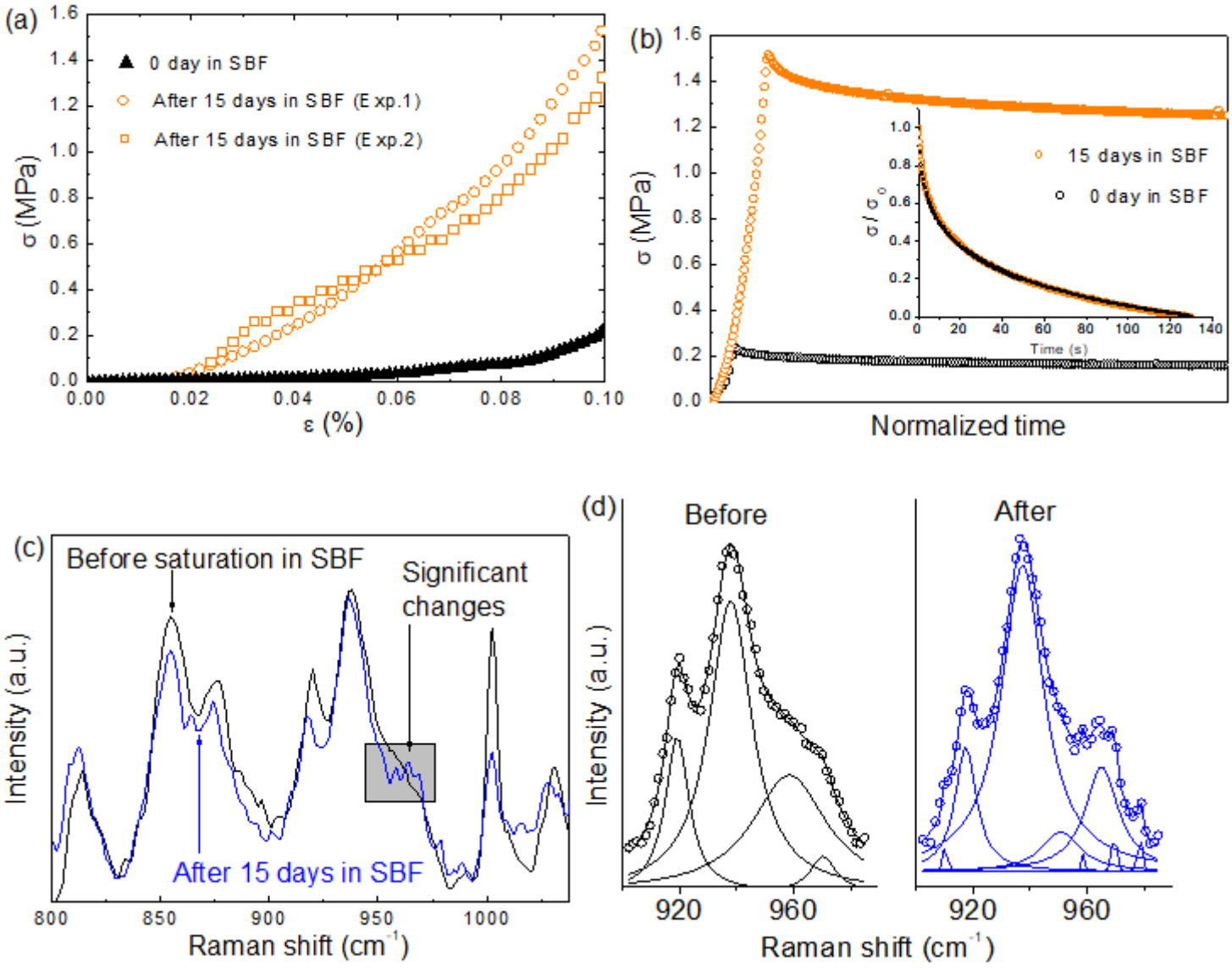

Figure 5- Comparison of stress and strain (a) and stress relaxation (b) of TMJ#2 samples before and after 15 days of incubation in a saturated simulated body fluid SBF and their respective Raman spectra (c); deconvolution of Raman spectra before (black) and after (blue) the incubation process (d) at the region with significant changes (baseline has been corrected linearly).

3.3 Effects of the chemical environment on mechanical properties and Raman spectra

The chemical environment of inflammation to the tissue was created by changing the chemical nature of the biological fluid in the device. Figures 6.a and 6.b show the evolution of the O_2 concentration and pH of the tissue bath in the bioreactor for the stable biological environment and during the oxidative process, respectively. The chemical modification resulted in an increase in the pH and a decrease in the O_2 content of the biological environment. Thus, the mechanical properties of the TMJ disc were obtained for different periods of the oxidative process, e.g., 1 minute, 10 hours and 2 days. Figure 6.c shows the comparison of the force as function of time during mechanical tension followed by stress relaxation of TMJ samples after different periods in corrosive environment and after fluid renewal. The modifications in the chemical environment lead to drastic modifications of the mechanical properties of the tissue as observed by the increase in force-relaxation depending on the time of exposure to the fluid. Figure 6.d shows the forces as a function of time after a renewal of the oxidative biological environment. The slight decrease in the force-relaxation after biological fluid renewal indicates a tissue performance stabilization. However, our experiments were not capable to detect a significant recovery (reversible process) in the mechanical properties with the samples used in this study. More experiments are needed to contest or corroborate the level of mechanical properties reversibility in a TMJ disc. Figure 6.d shows the Raman spectra of oxide TMJ disc exhibiting luminescence effects, that is, the characteristic peaks of the macromolecular structure are suppressed by the chemical interactions between the oxidative environment and biomolecules present on the tissue surfaces. These effects are characteristic of the formation of chemical groups that exhibit a two-photon absorption capability with collective excitations and a wide range of vibrational modes[35]. Therefore, the chemical modification of the biological environment leading to the production of oxidizing species around the tissue is evident.

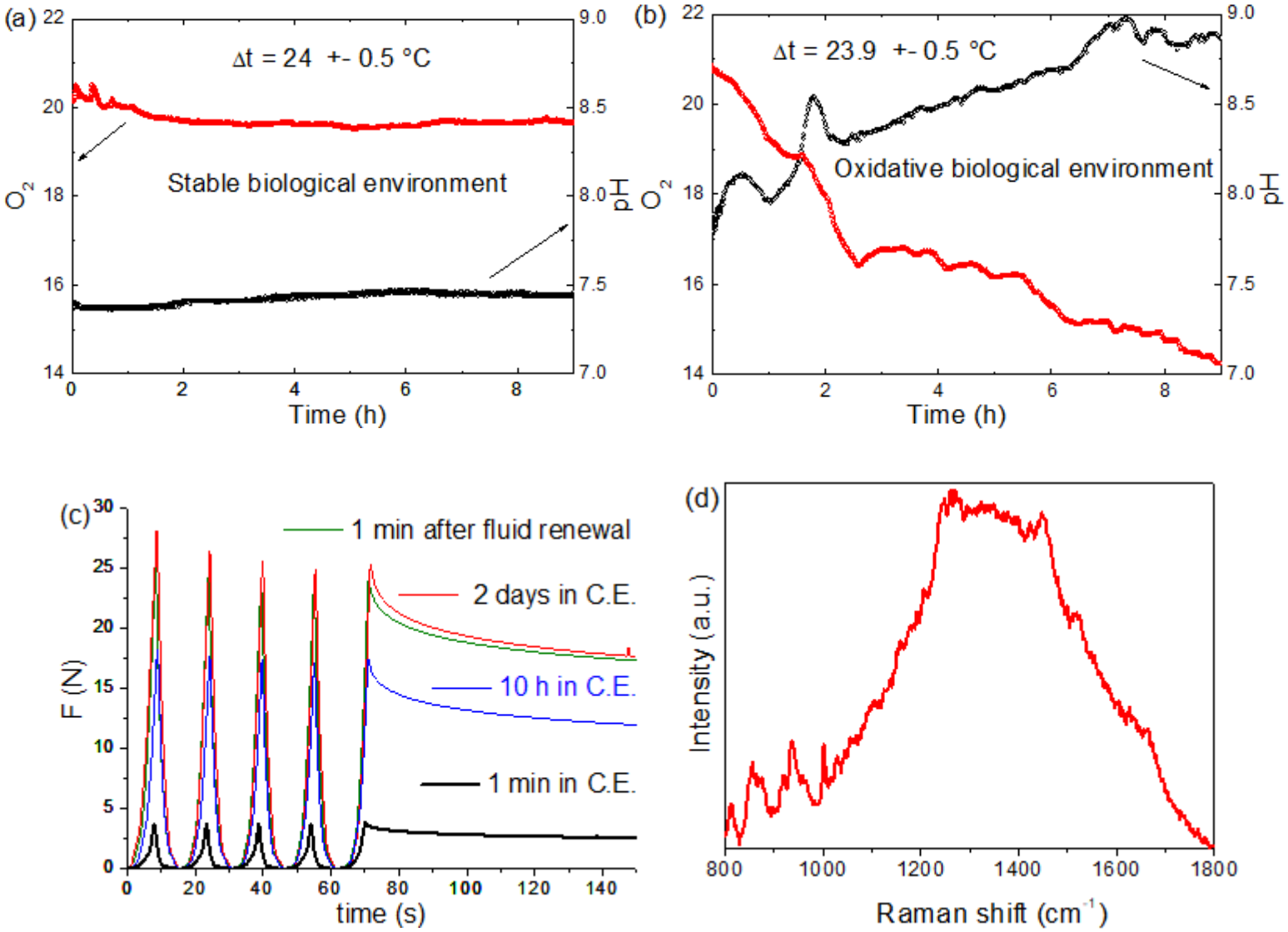

Figure 6- Evolution of the O_2 concentration and pH of the tissue bath with a stable biological environment (a) and the corrosive biological environment (b) in function of time. Comparison of the force as function of time during mechanical tensile load followed by stress relaxation of TMJ samples after different periods in corrosive environment C.E and after fluid renewal (c). Microscopy image of oxide TMJ disc and its respective Raman spectra (d).

3.4 Molecular mapping and statistical analysis of major contributors in mechanical tensile load

Confocal microscopy and Raman mapping were undertaken before and after mechanical loading. The beginning of the spectral mapping acquisition coincides with the end of the relaxation process to avoid micro movements. From the microscopy imaging, it is difficult to observe significant

morphological changes at the limit of the scale level of the lens (optical imagens of such observations are provided in fig. 2 of the supplementary material). Therefore, PCA analysis was conducted on the spectral data obtained after a normalization treatment. One-dimensional PCA-loadings plot in the 800-1800 cm^{-1} range of the Raman spectra was made for the TMJ disc before and after Mechanical Stressing (M.S.), respectively, and are provided in supplementary material. Considering the loadings of principal components, one can notice that variations in different spectral ranges are present. PCA1 and PCA2 components for both cases (with and without M.S.) seem to reflect mostly the intensity variations among spectra at different frequency ranges. Relatively small variations are reflected by PCA2, PCA3 and PCA4 components. It must be mentioned that each principal component can represent the superposition of different variations simultaneously and it is difficult to distinguish the variation of each Raman line. For that, it is possible to extract main Raman lines from the whole spectra and to carry out PCA analysis separately. In our case, particular attention can be given to the Raman line at 1000 cm^{-1}. Thus, the PCA analysis was also conducted only for a range around 1000 cm^{-1} in order to obtain only the variation of this line. Figure 7.a show the results of the PCA scores and loadings obtained from x,y profiles and one-dimensional PCA-loadings plot performed on the 900-1015 cm-1 spectral range (including, therefore, breathing mode) before M.S. One can notice that the loadings of the PCA1 component are the first derivative of the mentioned Raman line. This means that the PCA1 component reflects the variation of the position (Raman shift) of the mentioned band [36]. This behaviour is linked to the re-arrangement of the breathing mode of the phenylalanine-aromatic amino acids. Looking at the scores of this component the frequency shifts are present between different horizontal zones and the highest shift is for the upper zone, possibly attributed to molecular alignment in collagen fibre. The loadings of the PCA2 component looks like the measured Raman line of the breathing mode. This means that the PCA2 component reflects the variation of the intensity of this band and the apparition of the second band near 1012 cm^{-1} while PCA3 exhibits no representative variation.

In Figure 7.b the PCA scores and loadings are presented for the breathing mode for spectra obtained after M.S. In this configuration, the PCA1 component reflects the frequency shift of the breathing mode. Indeed, the PCA3 component looks like the second derivative of the band and that means this component

reflects the linewidth variation of the band. This variation was not observed in results obtained before M.S. Linewidth of Raman line is attributed to the amortization of the vibration and depends on any disorder in studied material. By applying mechanical stress, interatomic distances are modified which leads to the linewidth variation. In the scores image of PCA3 there are zones that undergo higher linewidth variations. The results pinpoint the major significant role of Raman the line at 1000 cm^{-1} as an omnipotent indicator of the TMJ disc response to the mechanical loading.

Before M.S.

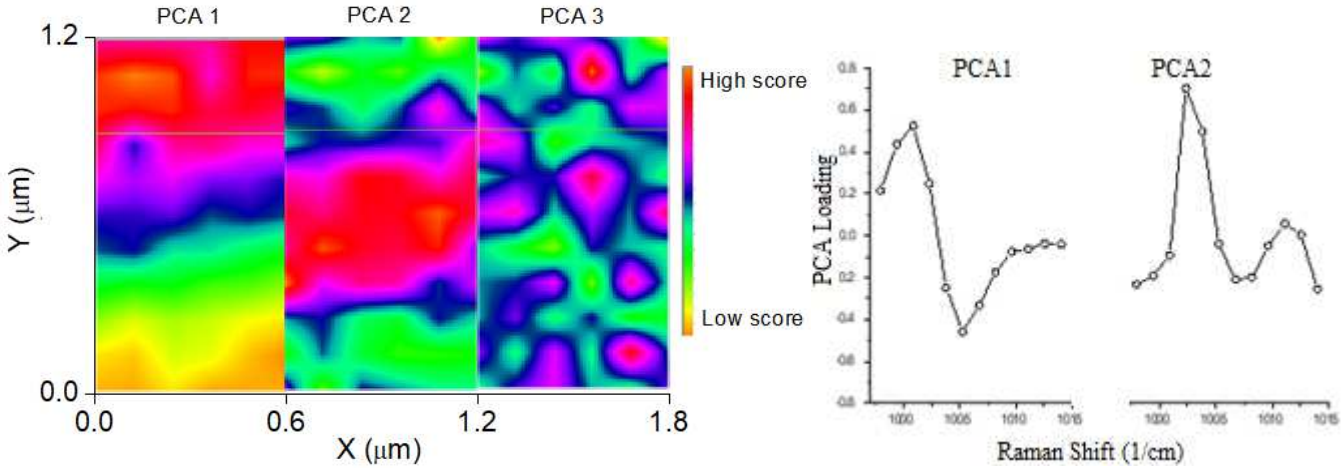

After M.S.

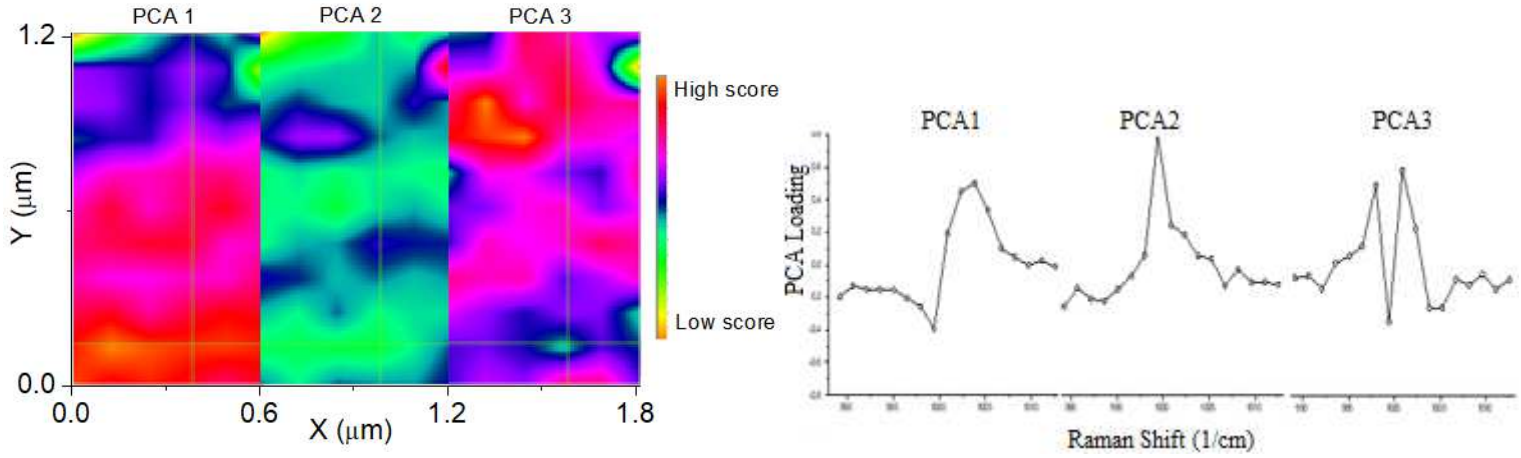

Figure 7- Results of PCA scores obtained from x,y profiles and one-dimensional PCA-loadings plot performed on the 900-1015 cm^{-1} spectral map of TMJ disc samples before and after M.S.

4. DISCUSSION

The mechanical characterization under quasi-static condition of the TMJ disc regarding the role of specific biomolecules considering the biochemical environment is crucial in order to perform suitable realistic simulations concerning properties that might lead to a premature dysfunction. In this work, this concern was experimentally assessed by a new homemade device, which allowed conducting vibrational spectroscopy while simultaneously applying tensile load with changes in the chemical environment. In order to reproduce the kinematics of the daily mechanical stress, the TMJ disc samples were preconditioned in cycles based on displacement field of a real movement of a human TMJ disc. The quantitative analysis of force versus displacement performed on TMJ disc samples revealed a modification of the mechanical properties of the preserved sample compared with a fresh one. Thus, the individual values of elastic modulus are no longer comparable. The contrast between values obtained by uniaxial stress tests on TMJ disc samples has already been reported. For further information concerning this controversy in elastic modulus values, we refer our readers to recent studies by Angelo et al [37] and Matuska et al [38]. In fact, the values of Young's modulus do not provide accurate information because their depends on different factors, such as strain rate, shape of the cut, direction of the tests, testing region, the method of preserving the samples, etc. In this way, we have opted to adopt an approach capable of suppressing these effects, that is, the mechanical-chemical coupling of the samples occurred in the same sample, modifications of which all occurred inside the device without external interference. This aspect was particularly crucial for molecular mapping with the objective of evaluating significant variations in molecular groups before and during the mechanical load.

A seldom-explored parameter of the mechanical properties of the TMJ disc is the effects of the modification of the biochemical environment on a tissue. An extremely useful application based on our suggested MC coupling approach is in using biological environment (in or case, SBF) while the Raman mapping is obtained from tissue under the daily mechanical loading. From the tensile test, an increase in the elastic modulus has been observed and attributed to the incubation process of the tissue in SBF. The revelation of additional peaks in the 950-980 cm^{-1} regions indicates the formation of a phosphate band ($\nu_1 PO_4^{3-}$), which is characteristic of carbonated apatites. Studies have suggested that the exact

position in this region is sensitive to mineral carbonate (CO_3^{2-}) and monohydrogen phosphate (HPO_4^{2-}) as well [39, 40]. The high HPO_4^{2-} content can shift this band to a lower wavenumber content. The possible cause for the formation of the new phases (amorphous apatites and/or some crystals) in tissue is the electrostatic attraction between positive ions from SBF and negative charge of tissue components, such as Proteoglycans observed at 1375 cm^{-1} region of the Raman spectra (Figure 3.a). Similar phenomenology has been observed in the interaction between positive ions, such as Ca^{2+} from SBF, and negatively charged proteins of biomembranes submitted to the same incubation process [41]. A certain level of the negative surface charges is responsible for the adsorption of Ca^{2+} from SBF. Therefore, the inorganic components are embedded in the TMJ disc by ionic bonds. The biological fluid contains varying amounts of cations and anions responsible for tissue regeneration-mineralization. However, calcium phosphates aggregated on the TMJ disc can reduce the ability of the cartilage to support mechanical loads and our MC coupling approach was able to assess this concern by identifying the Raman shift window at 900-980 cm^{-1} (Figure 5) as a key mediator related to calcium absorption in affecting the mechanical properties of the TMJ disc.

Another striking feature observed in this study concerns the influence of an oxidative chemical environment on the mechanical properties of the TMJ disc. Herein, an increase in stress-relaxation and luminescent effects have been observed (Fig. 6.c and 6.d) and attributed to its interaction with new chemical groups formed during the oxidative process near the tissue. The modification in the mechanical properties of the TMJ disc in different levels of the oxidative process indicate a time dependence. There are several practical consequences on tissue performance due to a high increase in elastic modulus as a consequence of oxidation. By pH changes as an example, the concentrations of hydrogen in body fluids can significantly affect the mechanical performance, that is, tissues suffer when the pH in body fluids rises too high. On the other hand, a rise in pH increases the influx of calcium into tissues, which also increases the elastic modulus. From mineralization and oxidation experiments, the results put in evidence the important role of the metabolically driven processes on the mechanical properties of the tissue, linking the biomechanical-biochemical effects.

Useful applications, based on our proposed approach, are in assessing the mechanical-chemical

coupling effects of the tissue with modification of the biological environment. The question remains, however: how do molecular groups respond to mechanical stress? According to molecular observations (Fig.3), the chemical groups observed in the 800-1050 cm^{-1} spectral region can be the key players in this process, which could be either individually or simultaneously modified under the mechanical load. We have hypothesized that the chemical heterogeneity is not negligible along fibril dimensions i.e., 4 μm^2. As aforementioned, strain induces shifts in vibrational frequencies. However, the results obtained from a couple of spectra is not enough to compute the all significant variations necessitating, therefore, the development of more accurate and appropriate statistical analysis that considers plausible complexity of tissue. Hence, PCA mathematical procedure was applied to the original Raman in order to obtain the main molecular modifications during the mechanical load. PC-loadings were plotted as a function of the variables related to regions with a different profile. Decoupling the major contributors in the mechanical loading-molecular response process, resulted in the identification of a major effector: breathing mode of the phenylalanine-aromatic amino acids. We suggest that future experimental studies on biomechanics of TMJ discs refer to Raman mapping followed by normalizations and statistical PCA analysis rather than gross Raman Spectra, and the quantification of this Raman Region, as important predictors of tissue response. Taken together, this suggested MC coupling approach is able to identify key molecular mediators in the mechanical loading of TMJ discs. Our coupled bioreactor-vibrational spectroscopy approach proved to be a powerful technique to guide tissue engineering because it provides a complete exploration of the tissue behaviour from macro to molecular level with control of the chemical environment. Furthermore, other phenomena could be studied applying this approach, for example, the modifications of viscoelastic properties as a function of osmosis rate modified by changes in the different components of biological fluids. In addition, a study of MC Chemical coupling effects as a function of different tissue disorders could be of great interest for a wide audience in medical fields. Under a material science perspective, other kind of biological material could be studied, such as other cartilages, bones, natural membranes and scaffolds for regenerative therapy.

5. SUMMARY

This manuscript reported an experimental study of Temporomandibular Joint disc by a new

homemade device that enables *in situ* molecular investigation of tissues with modification of the biological environment. The approach is able to reproduce the daily mechanical loading and identify the main molecular groups responsible for recovery of the dissipated energy during the stress, such as the breathing mode of the phenylalanine-aromatic amino acids. By linking biomechanical-biochemical aspects, the results show that both mineralization and oxidation process around the TMJ disc (related to current problems in cartilages) lead to significant modifications to mechanical properties of the tissue putting in evidence the important role of the chemical environment in tissue performance. The experimental bench proposed for the study of TMJ disc, simulating real conditions and followed by statistical PCA analysis, can offer new insights for a thorough analysis of the tissue behaviour, predicting common disorders and their causes.

ACKNOWLEDGEMENTS

The authors acknowledge the financial support provided by the Brazilian Agency FAPESP, grant numbers 2013/21970-8 and 2017/03842-3 and all technical team of the Mécanique des Matériaux, des Structures et du Vivant, LEM3 for all support, in particular, Sr. Pascal THOMANN and Sr. Frank DEMEURIE.

CONFLICT OF INTEREST

The authors declare no conflict of interest.

REFERENCES

[1] V.P. Willard, L. Zhang, K.A. Athanasiou, Tissue engineering of the temporomandibular joint, Comprehensive Biomaterials, Elsevier 5 (2011) 221–235.

[2] K.A. Athanasiou, A.J. Almarza, M.S. Detamore, K.N. Kalpakci, Tissue engineering of temporomandibular joint cartilage, Synthesis Lectures on Tissue Engineering 1 (2009) 1–122.

[3] M. Singh, M.S. Detamore, Tensile properties of the mandibular condylar cartilage, J Biomech Eng. 130(1) (2008) 011009.

[4] G.R. Snider, J. Lomakin, M. Singh, S.H. Gehrke, M.S. Detamore, Regional dynamic tensile properties of the TMJ disc. J Dent Res 87(11) (2008) 1053-1057.

[5] S. Fazaeli, S. Ghazanfari, V. Everts, T. Smit, J. Koolstra, The contribution of collagen fibers to the mechanical compressive properties of the temporomandibular joint disc, Osteoarthritis and Cartilage 24(7) (2016) 1292 – 130.

[6] P. Fernández, M. J. Lamela, A. Ramos, A. Fernández-Canteli, E. Tanaka, The region-dependent dynamic properties of porcine temporomandibular joint disc under unconfined compression, Journal of Biomechanics 46(4) (2013) 845 – 848.

[7] E. Tanaka, N. Kawai, M. Tanaka, M. Todoh, T. Van Eijden, K. Hanaoka, The frictional coefficient of the temporomandibular joint and its dependency on the magnitude and duration of joint loading. J Dent Res. 83(5) (2004) 404-407.

[8] J.C. Nickel, L.R. Iwasaki, M.W. Beatty, M.A. Moss, D.B. Marx, Static and dynamic loading effects on temporomandibular joint disc tractional forces. J Dent Res. 85(9) (2006) 809-813.

[9] G.A. Zarb, G.E. Carlsson, Temporomandibular disorders: osteoarthritis. J Orofac Pain, 13(4) (1999) 295-306.

[10] M. Jibiki, S. Shimoda, Y. Nakagawa, K. Kawasaki, K. Asada, K. Ishibashi, Calcifications of the disc of the temporomandibular joint. J Oral Pathol. Med 28(9) (1999) 413-419.

[11] E. Tanaka, M.S. Detamore L.G. Mercuri, Degenerative disorders of the temporomandibular joint: etiology, diagnosis, and treatment. J Dent Res. 87(4) (2008) 296-307.

[12] A.J. Almarza, A.C. Bean, L.S. Baggett, K.A. Athanasiou, Biochemical analysis of the porcine temporomandibular joint disc. Br J Oral Maxillofac Surg. 44(2) (2006) 124-128.

[13] M. Fuerst, O. Niggemeyer, L. Lammers, F. Schäfer, C. Lohmann, W. Rüther. Articular cartilage mineralization in osteoarthritis of the hip. BMC Musculoskeletal Disorders 10 (2009) 166.

[14] H. Sano, Y. Saijo and S. Kokubun, Non-mineralized fibrocartilage shows the lowest elastic modulus in the rabbit supraspinatus tendon insertion: Measurement with scanning acoustic microscopy. J Shoulder Elbow Surg. (2006) 743-749.

[15] M. L. Roemhildt, B. D. Beynnon, M. Gardner-Morse. Mineralization of Articular Cartilage in the Sprague-Dawley Rat: Characterization and Mechanical Analysis Osteoarthritis Cartilage 20(7) (2012) 796–800.

[16] Goldring MB. Articular cartilage degradation in osteoarthritis. HSS J. 2012;8:7–9

[17] John A. Hardin, Neil Cobelli, and Laura Santambrogio. Consequences of metabolic and oxidative modifications of cartilage tissue. Nat Rev Rheumatol. 2015 Sep; 11(9): 521–529.

[18] K. Chatzipanagi, C.G. Baumann, M. Sandri, S. Sprio, A. Tampieri, R. Kröger, In situ mechanical and molecular investigations of collagen/apatite biomimetic composites combining Raman spectroscopy and stress-strain analysis. Acta Biomaterialia 46 (2016) 278-285.

[19] A. Masic, L. Bertinetti, R. Schuetz, L. Galvis, N. Timofeeva, J. W. C. Dunlop, J. Seto, M. A. Hartmann and P. Fratz. Observations of Multiscale, Stress-Induced Changes of Collagen Orientation in Tendon by Polarized Raman Spectroscopy. Biomacromolecules 12(11) (2011) 3989–3996.

[20] R. Ramakrishnaiah, S. B. Kotha, A.A.A.Khuraif, S. L. Celur, D. D. Divakar, F. Javed, I. U. Rehman, Applications of Raman spectroscopy in dentistry part II: Soft tissue analysis, Applied Spectroscopy Reviews 51 (2016) 799-821.

[21] Shiyamala Duraipandian, Wei Zheng, Joseph Ng, Jeffrey J.H. Low, A. Ilancheran, and Zhiwei Huang. Simultaneous Fingerprint and High-Wavenumber Confocal Raman Spectroscopy Enhances Early Detection of Cervical Precancer In Vivo. Anal. Chem. 84, 14, 5913-5919 (2012).

[22] Mads Sylvest Bergholt, Wei Zheng, Khek Yu Ho, Ming Teh, Khay Guan Yeoh, Jimmy Bok Yan So, Asim Shabbir, Zhiwei Huang. Fiberoptic Confocal Raman Spectroscopy for Real-Time In Vivo Diagnosis of Dysplasia in Barrett's Esophagus, Gestroenterology 146, 1, 27–32 (2014).

[23] F. J. González J. Alda B. Moreno ‐ Cruz M. Martínez ‐ Escanamé M. G. Ramírez ‐ Elías B. Torres ‐ Álvarez B. Moncada. Use of Raman spectroscopy for the early detection of filaggrin ‐ related atopic dermatitis. Skin Res. and Technolog. 17, 1, 45-50 (2011).

[24] A. Bermejo, O. González, J. González, The pig as an animal model for experimentation on the temporomandibular articular complex, Oral Surgery, Oral Medicine, Oral Pathology 75(1) (1993) 18 – 23.

[25] M. S. Detamore, K.A. Athanasiou, Tensile properties of the porcine temporomandibular joint disc, Journal of Biomechanical Engineering 125(4) (2003) 558–565.

[26] K.W. Kim, M.E. Wong, J. F. Helfrick, J. B. Thomas, K.A. Athanasiou, Biomechanical tissue characterization of the superior joint space of the porcine temporomandibular joint, Annals of Biomedical Engineering 31(8) (2003) 924–930.

[27] D. K. Pattanayak, S. Yamaguchi, T. Matsushita, T. Nakamura, T. Kokubo. Apatite-forming ability of titanium in terms of pH of the exposed solution, Soc. Interface 9 (2012) 2145–2155.

[28] Eriksson, P. L. Westesson. J. Oral Surgey 59 (1985) 449-452.

[29] J.E. Jackson, Hoboken, A User's Guide to Principal Components Analysis, NJ: John Wiley&Sons (2003).
[30] I.T. Jolliffe, Principal Component Analysis, Springer Series in Statistics (2002).
[31] T.R. Brown, R. Stoyanova, J. of Magnetic Resonance B 112, 31 (1996).
[32] H. Witjes, M. van den Brink, W.J. Melssen, L.M.C. Buydens, Chemometrics and Intelligent Laboratory Systems 52, (2000) 105.

[33] Tappert, L.K., Baldit, A., Rahouadj, R., and Lipinski P. Local elastic properties characterization of the temporo-mandibular joint disc through macro-indentation. Computer Methods in Biomechanics and Biomedical Engineering, 20 (2017) 201-202.

[34] G,Penel, C,Delfosse M,Descamps, G. Leroy, Composition of bone and apatitic biomaterials as revealed by intravital Raman microspectroscopy, Bone 36 (2005) 893–901.

[35] M. Drobizhev, N. S. Makarov, S. E. Tillo, T. E. Hughes, A. Rebane, Two-photon absorption properties of fluorescent proteins. Nat. Methods 8 (2011)393 –399.

[36] N. Kokanyan, D. Chapron, E. Kokanyan, M.D. Fontana. Zr doping on lithium niobate crystals: Raman spectroscopy and chemometrics. Journal of Applied Physics 121 (2017) 095103.

[37] D. Angelo, P. Morouço, N. Alves, T. Viana, F. Santos, R. González, F. Monje, D. Macias, B. Carrapiço, R. Sousa, S. Cavaco-Gonçalves, F. Salvado, C. Peleteiro, M. Pinho, Choosing sheep (ovis aries) as animal model for temporomandibular joint research: Morphological, histological and biomechanical characterization of the joint disc', Morphologie 100(331) (2016) 223 – 233.

[38] A.M. Matuska, S. Muller, M. Dolwick, P. S. McFetridge, Biomechanical and biochemical outcomes of porcine temporomandibular joint disc deformation, Archives of Oral Biology 64 (2016) 72 – 79.

[39]] N.J. Crane, V. Popescu, M.D. Morris, P. Steenhuis, M.A. Ignelzi, Jr. Raman spectroscopic evidence for octacalcium phosphate and other transient mineral species deposited during intramembranous mineralization. Bone, 39 (2006) 434–442

[40] A. Awonusi, M.D. Morris, M.M.J. Tecklenburg, Carbonate assignment and calibration in the Raman spectrum of apatite. Calcif Tissue Int. 81 (2007) 46–52. [41] P.N, Hirschmann, C.A. Shuttleworth. The collagen composition of the mandibular joint of the fetal calf. Arch Oral Biol. 21(12) (1976) 771-773.

[41] R.M. Nascimento, S.M.M, Ramos, I.H. Bechtold, A.C. Hernandes, Wettability Study on Natural Rubber Surfaces for Applications as Biomembranes. ACS Biomaterials Science & Engineering, 4 (2018) 2784-2793.

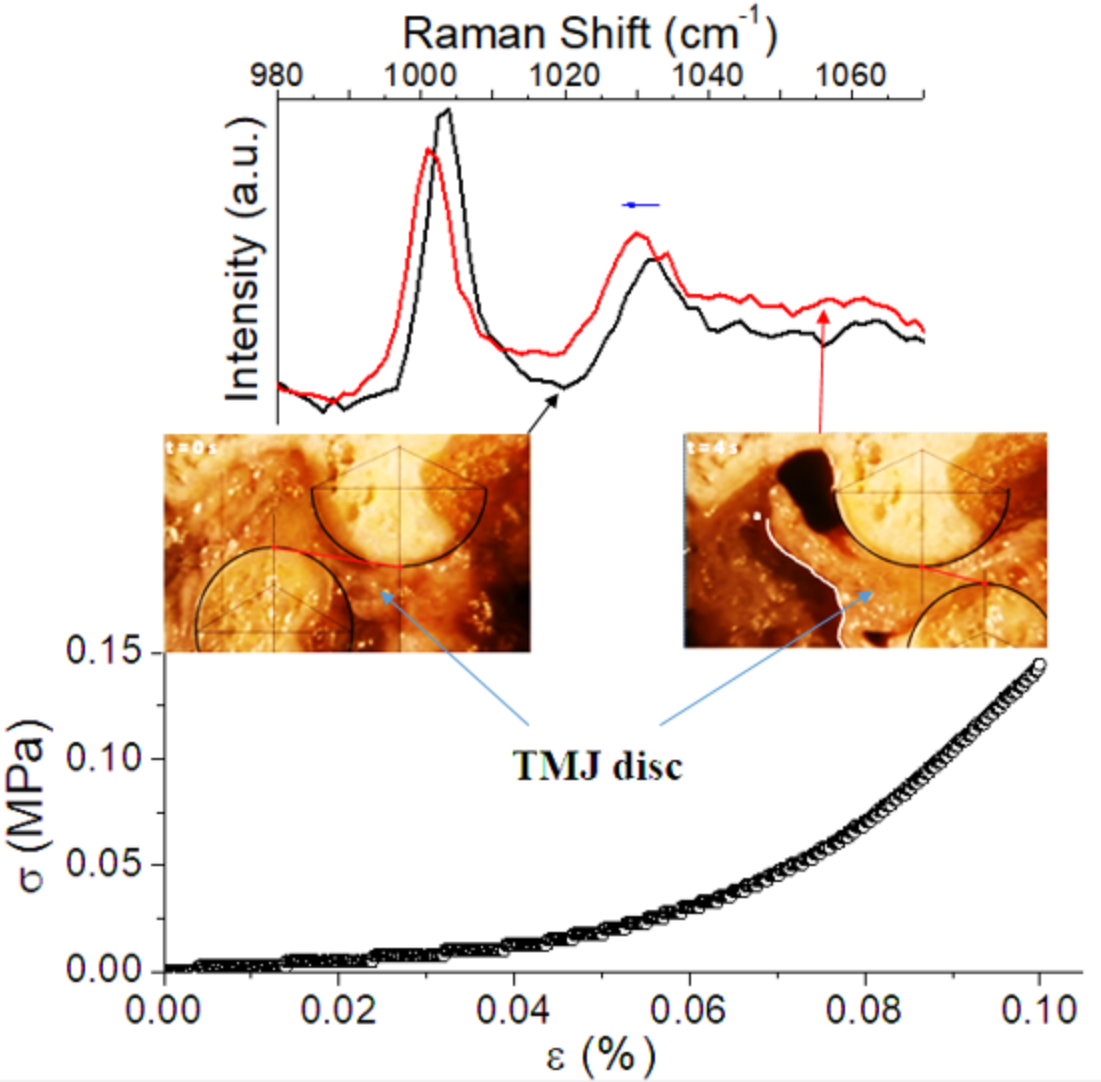
Raman Shift (cm-1)
980
1000
1020
1040
1060
Intensity (a.u.)
t=0s
t=4s
TMJ disc
0.15
0.10
0.05
0.00
σ (MPa)
0.00
0.02
0.04
0.06
0.08
0.10
ε (%)